



Photochemical oxidative decolorization of C. I. basic red 46 by UV/H₂O₂ process: Optimization using response surface methodology and kinetic modeling

A.R. Khataee^a, B. Habibi^{b,*}

^aDepartment of Applied Chemistry, Faculty of Chemistry, University of Tabriz, Tabriz, Iran
Tel. +98 411 3393165; email: a_khataee@tabrizu.ac.ir; ar_khataee@yahoo.com

^bElectroanalytical Chemistry Laboratory, Department of Chemistry, Faculty of Sciences, Azarbaijan University of Tarbiat Moallem, Tabriz, Iran
email: b.habibi@azaruniv.edu

Received 11 August 2009; Accepted 7 December 2009

ABSTRACT

In this work Central Composite Design (CCD) based on Response Surface Methodology (RSM) was employed to evaluate the effects of operational parameters (reaction time, initial dye concentration, initial H₂O₂ concentration and distance of UV lamp from the solution) affecting photooxidative decolorization of a dye solution containing C.I. Basic Red 46 (BR46) and for optimization of the process. Predicted values were found to be in good agreement with experimental values ($R^2 = 98.92\%$ and $Adj-R^2 = 97.79\%$), which indicated suitability of the model employed and the success of CCD in optimizing the conditions of UV/H₂O₂ process. Graphical response surface and contour plots were used to locate the optimum point. The results of optimization predicted by the model showed that maximum decolorization efficiency was achieved at the optimum condition of reaction time 14 min, initial dye concentration 20 mg/L, initial H₂O₂ concentration 1.0 g/L and 16 cm distance between UV lamp and the solution. In addition, a mathematical relation between the apparent reaction rate constant and used H₂O₂ was applied for prediction of the photooxidative decolorization rate constant (k). The results indicated that this kinetic model provided good prediction of the k values for a variety of conditions. The Figure-of-merit electrical energy per order (E_{Eo}) was employed to estimate the electrical energy consumption.

Keywords: Advanced oxidation processes; Central composite design; Modeling; Electrical energy consumption; Decolorization.

1. Introduction

Textile industries discharge large amounts of colored wastewaters due to the unfixed dyes on fibers during the coloring and washing steps. The presence of these pollutants in water streams causes problems related to their carcinogenicity, toxicity to aquatic life and the easily detected

and undesirable aesthetic aspect [1–4]. Dyeing effluents are very difficult to treat, due to their resistance to biodegradability, stability to light, heat and oxidizing agents [5–7]. In general, the treatment of dye-containing effluents is being undertaken by biological, adsorption, membrane, coagulation–flocculation, oxidation–ozonation, biological and advanced oxidation processes (AOP_s) [8–11]. AOP_s have been developed to degrade the nonbiodegradable contaminants of drinking water and industrial effluents into harmless species (CO₂, H₂O, etc.) [12]. Combined UV

*Corresponding author.

and hydrogen peroxide oxidation, is one of the advanced oxidation processes which has been successfully applied to the treatment of various water pollutants. This process implies such simple reactions as UV photolysis of H_2O_2 . It is characterized by the generation of a very powerful oxidizing species, well known as hydroxyl radicals, in relative high steady-state concentrations. These reactive radicals can decompose and even mineralize the organic contaminants with high efficiency. The main advantages of this process are that no additional disposal problems are generated after the completion of the above treatment and they are non-selective to a very broad range of chemicals. Reaction scheme of the proposed mechanism for UV/ H_2O_2 process has been summarized in the following equation [13–16].

1.1. Initiation

(The typical molar extinction coefficient and primary quantum yield of direct photolysis of hydrogen peroxide are $18.6 \text{ dm}^3 \text{ mol}^{-1} \text{ cm}^{-1}$ and 0.5 mol E^{-1} at 254 nm, respectively [15]):



1.2. Hydroxyl radical propagation and termination



1.3. Overall reaction



As we have reported in our previous papers [13,14,17], the photooxidative decolorization efficiency is dependent on various parameters such as oxidant (H_2O_2) amount, initial dye concentration, UV radiation intensity, reaction time and initial pH. In order to determine the influence of these parameters in conventional methods, experiments were carried out varying systematically the studied parameter and keeping constant the others. This should be repeated to all the influence parameters, resulting in an unreliable number of experiments. In addition, this exhaustive procedure is not able to find combined effect of the effective parameters. In order to optimize the effective parameters

with the minimum number of experiments, application of the experimental design methodologies can be useful. The common experimental design techniques used for process analysis are full factorial, partial factorial and response surface methodology. A full factorial requires at multilevel many experiments [18]. A partial factorial design requires fewer experiments than a full factorial. However the former is particularly useful if certain variables are already known to show no interaction [19,20]. An effective alternative to the factorial design is the response surface methodology. RSM is an experimental design technique that uses mathematical and statistical techniques to analyze the influence of independent variables on a specific dependent variable (response) [21]. Using RSM, it is possible to estimate linear, interaction and quadratic effects of the factors and to provide a prediction model for the response. In this way, RSM designs could be used to find improved or optimal process settings in an efficient use of the resources. Experimental data required are dependent on the chosen design, central composite or box–Behnken designs [22]. These are different in the number of runs required and in the combinations of the levels used in the experiments. The central composite design gives almost as much information as a multilevel factorial. It requires much fewer experiments than a full factorial. CCD has been also shown to be sufficient to describe the majority of steady-state process responses [23].

RSM methodology has been applied to model and optimize several wastewater treatment processes including adsorption [21,24], Fenton's oxidation [25,26], electrochemical oxidation [27], electrocoagulation [28] and photocatalytic decolorization [29]. However, to the best of our knowledge, the optimization of photooxidative decolorization of BR46 solution and the effect of interaction of effective parameters using central composite design have not been reported.

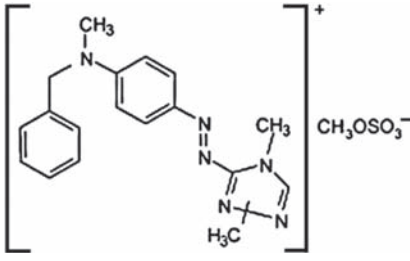
In this work, the central composite design has been applied to optimization of decolorization of a dye solution containing BR46 using UV/ H_2O_2 process. The factors (variables) investigated were the reaction time, initial dye concentration, initial H_2O_2 concentration and distance of UV lamp from the solution. In addition a kinetic model has been used to evaluate of the apparent rate constants (k), in terms of the ratio of initial concentration of H_2O_2 to that of the dye, in the photooxidative removal of BR46 using UV/ H_2O_2 process.

2. Experimental details

2.1. Reagents

Hydrogen peroxide (30%, $d = 1.11 \text{ g/mL}$), sulfuric acid and sodium hydroxide were of laboratory reagent grade (Merck Co.) and used without further purification. The dye, C.I. basic red 46, was obtained from Shimi

Table 1
Characteristics of C. I. Basic Red 46.

Molecular formula	$C_{18}H_{24}N_6O_4S$
Molecular mass	420 (g mol ⁻¹)
λ_{max}	530 (nm)
Other name	Maxilon Red GRL
Chemical Class	Cationic mono azo
Chemical structure	

Boyakhsaz Company, Iran. Its structure and characteristics are given in Table 1.

2.2. General procedure

For UV/H₂O₂ process, irradiation was carried out with a 30 W (UV-C) mercury lamp (Philips, the Netherlands), which was put above a batch photoreactor of 500 mL in volume. The desired concentration of BR46 and H₂O₂ were fed into the Pyrex reactor. The distance between the solution and UV source was adjusted according to the experimental conditions. On the surface of the solution, the radiation intensity was measured by Cassy Lab, Germany. The pH of the solution was measured by pH meter (Philips PW 9422, the Netherlands). The initial value of dye solution pH was 6.5. Then, the UV lamp was switched on to initiate the reaction. During irradiation, agitation was maintained to keep the solution homogeneous. At different reaction times obtained with experimental design, 2 mL sample were taken and the remaining BR46 was determined using a Lightwave S2000 UV/Vis spectrophotometer, England at $\lambda_{max} = 530$ nm and calibration curve. Using this method, the percent color removal

Table 2
Experimental ranges and levels of the independent test variables.

Variables	Ranges and levels				
	-2	-1	0	+1	+2
Reaction time (min) (X_1)	2	6	10	14	18
Initial dye concentration (mg/L) (X_2)	4	8	12	16	20
Initial H ₂ O ₂ concentration (g/L) (X_3)	0.2	1.2	2.2	3.21	4.2
Distance from UV lamp (cm) (X_4)	4	8	12	16	20

could be obtained. The percent color removal (CR (%)) was expressed as the percentage ratio of decolorized dye concentration to that of the initial one.

2.3. Experimental design

Response surface methodology is a collection of statistical and mathematical techniques useful for developing, improving and optimizing processes. The application of statistical experimental design techniques in the development of the photooxidative process can result in reduced process variability combined with the requirement of less resources (time, reagents and experimental work) [30].

In the present study central composite design, which is a widely used form of RSM, was employed for optimization of UV/H₂O₂ process. In order to evaluate the influence of operating parameters on the photooxidative decolorization efficiency of BR46, four main factors were chosen: reaction time (X_1), initial dye concentration (X_2), initial H₂O₂ concentration (X_3) and distance of UV lamp and solution (X_4). A total of 31 experiments were employed in this work, including $2^4 = 16$ cube points, 7 replications at the center point and 8 axial points. Experimental data were analyzed using Minitab 15 software. For statistical calculations, the variables X_i were coded as x_i according to the following equation:

$$x_i = \frac{X_i - X_0}{\delta X} \quad (9)$$

where X_0 is the value of X_i at the center point and δX presents the step change [31,32]. The experimental ranges and the levels of the independent variables for BR46 removal are given in Table 2. It should be mentioned that preliminary experiments was performed to determine the extreme values of the variables.

3. Results and discussion

3.1. Central composite design model

CCD involves the following steps: performing the statistically designed experiments according to the design, factors and levels selected, estimating the coefficients of the mathematical model to predict the response and check its adequacy [29, 31]. The 4-factor CCD matrix and experimental results obtained in the photooxidative color removal runs are presented in Table 3. The second-order polynomial response equation (Eq. (10)) was used to correlate the dependent and independent variables:

$$Y = b_0 + b_1x_1 + b_2x_2 + b_3x_3 + b_4x_4 + b_{12}x_1x_2 + b_{13}x_1x_3 + b_{14}x_1x_4 + b_{23}x_2x_3 + b_{24}x_2x_4 + b_{34}x_3x_4 + b_{11}x_1^2 + b_{22}x_2^2 + b_{33}x_3^2 + b_{44}x_4^2 \quad (10)$$

Table 3
The 4-factor central composite design matrix and the value of response function (CR%).

Run	Reaction time (min)	Initial dye concentration (mg/L)	Initial H ₂ O ₂ concentration (g/L)	Distance from UV lamp (cm)	Decolorization efficiency (%)	
					Experimental	Predicted
1	-1	1	1	1	32.00	32.63
2	1	-1	1	-1	76.10	77.29
3	2	0	0	0	72.50	72.66
4	1	1	-1	1	95.50	94.27
5	0	0	0	0	80.00	80.26
6	1	1	-1	-1	91.34	88.45
7	0	0	0	-2	89.00	90.40
8	1	-1	-1	-1	96.00	94.24
9	-1	-1	-1	1	71.00	65.97
10	1	-1	-1	1	75.00	78.97
11	0	0	0	2	60.00	58.36
12	-1	1	1	-1	48.00	47.39
13	-2	0	0	0	23.00	22.60
14	0	0	0	0	80.00	80.26
15	-1	1	-1	-1	70.00	68.51
16	-1	-1	1	1	10.00	16.25
17	0	-2	0	0	75.00	73.08
18	0	0	0	0	80.00	80.26
19	0	0	0	0	80.00	80.26
20	0	0	0	0	80.00	80.26
21	-1	1	-1	1	65.23	67.40
22	0	0	-2	0	95.00	96.74
23	1	1	1	0	74.25	74.62
24	1	1	1	-1	82.55	84.45
25	0	2	0	0	80.00	81.68
26	0	0	0	0	80.00	80.26
27	-1	-1	-1	-1	85.18	88.17
28	-1	-1	1	-1	56.00	54.10
29	0	0	2	0	45.00	43.02
30	1	-1	1	1	48.00	46.36
31	0	0	0	0	81.82	80.26

where Y is a response variable of decolorization efficiency. The b_i are regression coefficients for linear effects; b_{ik} the regression coefficients for quadratic effects; x_i are coded experimental levels of the variables.

Based on these results, an empirical relationship between the response and independent variables was attained and expressed by the following second-order polynomial equation:

$$\begin{aligned}
 Y = & 80.2593 + 12.5135x_1 + 2.1490x_2 - 13.4315x_3 - 8.0083x_4 \\
 & - 8.1571x_1x_2 - 0.7196x_1x_3 - 2.5946x_1x_4 - 1.4696x_2x_3 \\
 & + 3.4683x_2x_4 + 4.2791x_3x_4 + 1.7323x_1^2 \\
 & + 3.2383x_2^2 + 5.2731x_3^2 - 3.9127x_4^2.
 \end{aligned} \quad (11)$$

The decolorization efficiencies (CR%) have been predicted by Eq. (11) and presented in Table 3. These results indicated good agreements between the experimental and predicted values of decolorization efficiency. In addition, Eq. (11) suggests that the coefficient b_{13} (-0.7196) is not significant and could be removed from the model equation.

3.2. Determination coefficients and residuals analysis

The regression coefficient (R^2) quantitatively evaluates the correlation between the experimental data and the predicted responses. Experimental results and the predicted values obtained using model (Eq. (11)) are shown in Fig. 1.

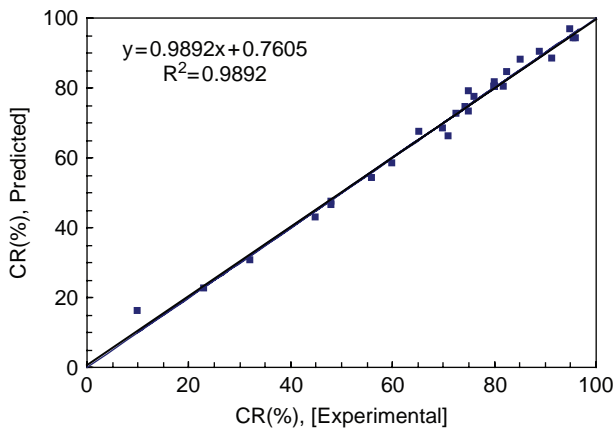


Fig. 1. Comparison of the experimental results of decolorization efficiency with those calculated via central composite design resulted equation.

Two lines were used to show the success of the prediction. The first line is the perfect fit (predicted data equal to experimental data), on which all the data of an ideal model should lay. The other line is the line that best fits on the data of the scatter plot with Eq. $Y = ax + b$ and it is obtained with regression analysis based on the minimization of the squared errors. The determination coefficient of this line is also presented (R^2). The closer to 1 this factor is and the closer the coefficients of the line to 1 and 0, respectively, are the better the model is. As can be seen, the predicted values match the experimental values reasonably well with R^2 of 0.9892.

The obtained R^2 value suggests good adjustments to the experimental results since this indicates that 0.9892 of the variability in the response could be explained by the models. This implies that 98.92% of the variations for percent color removal are explained by the independent variables and this also means that the model does not explain only about 1.08% of variation. Adjusted R^2 (Adj- R^2) is also a measure of goodness of a fit, but it's more suitable for comparing models with different numbers of independent variables. It corrects R^2 -value for the sample size and the number of terms in the model by using the degrees of freedom on its computations. If there are many terms in a model and not very large sample size, adjusted R^2 may be visibly smaller than R^2 [21, 22]. Here, adjusted R^2 value (0.9779) was very close to the corresponding R^2 value (see Table 4).

In addition to regression coefficient, the adequacy of the models was also evaluated by the residuals (difference between the observed and the predicted response value). Residuals are thought as elements of variation unexplained by the fitted model and then it is expected that they occur according to a normal distribution. Normal probability plots are a suitable graphical method for judging the normality of the residuals. The observed residuals are plotted against the expected values, given by a normal distribution (see Fig. 2). The residuals from the analysis should be normally distributed. In practice, for balanced or nearly balanced designs or for data with a large number of observations, moderate departures from normality do not seriously affect the results. The normal probability plot of the residuals should roughly follow a straight line. Trend observed in Fig. 2(a), reveals reasonably well-behaved residuals. Fig. 2(b) shows the residuals versus the fitted values. Based on this plot, the residuals appear to be randomly scattered about zero. Fig. 2(c) and (d) illustrate the residuals in the order of the corresponding observations and the histogram of the residuals distribution. It shows that the residuals in the plot fluctuate in a random pattern around the line of error zero.

3.3. Analysis of variance

Table 4 indicates the results of the quadratic response surface model fitting in the form of analysis of variance (ANOVA). ANOVA is required to test the significance and adequacy of the model [33, 34]. ANOVA subdivides the total variation of the results in two components: variation associated with the model and variation associated with the experimental error, showing whether the variation from the model is significant or not when compared with the ones associated with residual error [21, 32, 35]. This comparison is performed by F -value, which is the ratio between the mean square of the model and the residual error. If the model is a good predictor of the experimental results, F -value should be greater than the tabulated value of F -distribution for a certain number of degrees of freedom in the model at a level of significance α . F -value obtained, 104.41, is clearly greater than the tabulated F (2.352 at 95% significance) confirming the adequacy of the model fits.

Table 4
Analysis of variance (ANOVA) for fit of decolorization efficiency from central composite design.

Source of variations	Sum of squares	Degree of freedom	Adjusted Mean square	F -value
Regression	13127.1	14	937.65	104.41
Residuals	143.7	16	8.98	
Total	13270.8			

$R^2 = 98.92\%$, Adjusted $R^2 = 97.79\%$.

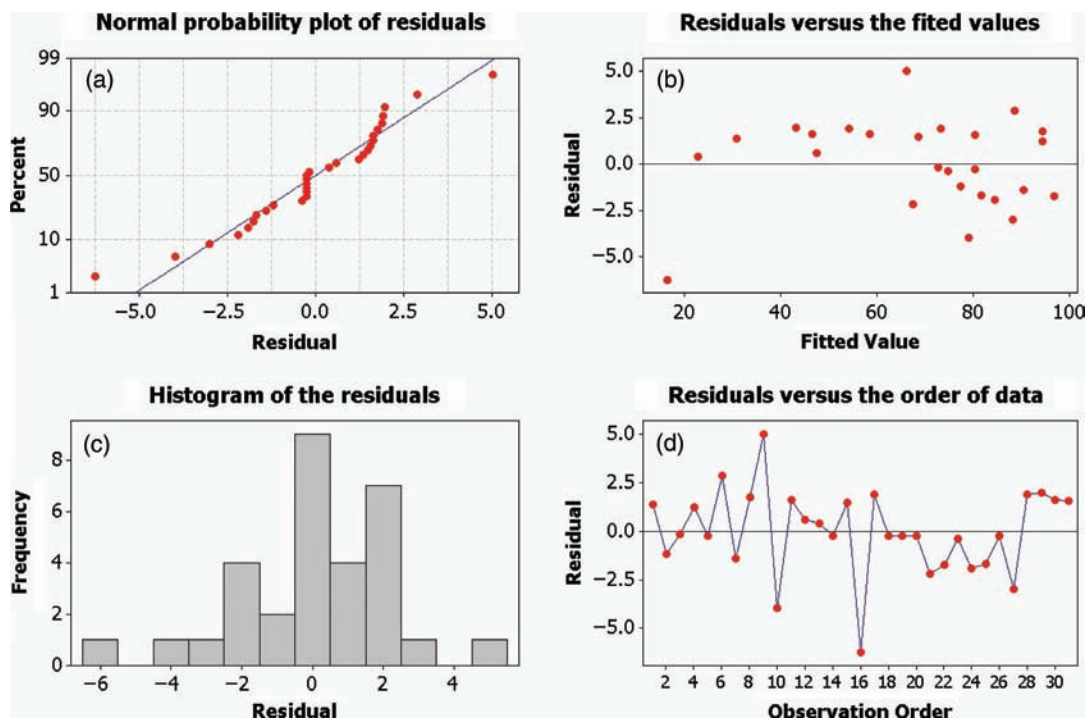


Fig. 2. Residual plots for photooxidative decolorization efficiency of BR46.

The student's t distribution and the corresponding values, along with the parameter estimate, are given in Table 5. The P -values were used as a tool to check the significance of each of the coefficients, which, in turn, are necessary to understand the pattern of the mutual interactions between the test variables. The larger the magnitude of the student's t -test and smaller P -value, the more significant is the corresponding coefficient [31,32].

3.4. Effect of variables as response surface and counter plots

In order to gain insight about the effect of each variable, the three dimensional (3D) and contour (2D) plots for the predicted responses were formed. These plots are created based on the model polynomial function to analyze the change of the response surface. The surface and contour plots of the quadratic model with two variables kept constant and the other two

Table 5

Estimated regression coefficients and corresponding t and P -values from the data of central composite design experiments.

Coefficient	Parameter estimate	Standard error	t -value	P -value
b_0	80.2593	1.1326	70.860	0.000
b_1	12.5135	0.6117	20.457	0.000
b_2	2.1490	0.6117	3.513	0.003
b_3	-13.4315	0.6117	-21.958	0.000
b_4	-8.0083	0.6117	-13.092	0.000
b_{12}	-8.1571	0.5604	-14.556	0.000
b_{13}	-0.7196	0.5604	-1.284	0.217
b_{14}	-2.5946	0.5604	-4.630	0.000
b_{23}	-1.4696	0.5604	-2.622	0.018
b_{24}	3.4683	0.7492	4.630	0.000
b_{34}	4.2791	0.7492	5.712	0.000
b_{11}	1.7323	0.7492	2.312	0.034
b_{22}	3.2383	0.7492	4.323	0.001
b_{33}	5.2731	0.7492	7.039	0.000
b_{44}	-3.9127	0.7492	-5.223	0.000

varying within the experimental ranges are shown in Figs. 3–6.

Response surface plots provide a method to predict the percent color removal for different values of the tested variables and the contours of the plots help in identification of the type of interactions between these variables [36].

In Fig. 3, the response surface and contour plots were developed as a function of initial dye concentration and reaction time while the initial H₂O₂ concentration and distance of UV lamp from the solution were kept constant at 2.2 g/L and 12 cm, respectively, being the central levels. Fig. 3 shows a maximum for percent color removal as time increases especially for lower initial dye concentrations. The presumed reason is that at the beginning stages of the process, hydroxyl radicals attack to the dye molecules that results in increase of percent color removal. The reactions of $\cdot\text{OH}$ and $\cdot\text{O}_2\text{H}$ with dye molecules result in the formation of intermediates. The produced intermediates in solution may quench hydroxyl radicals which cause a decrease in percent color removal. In addition, when initial amount of H₂O₂ was kept con-

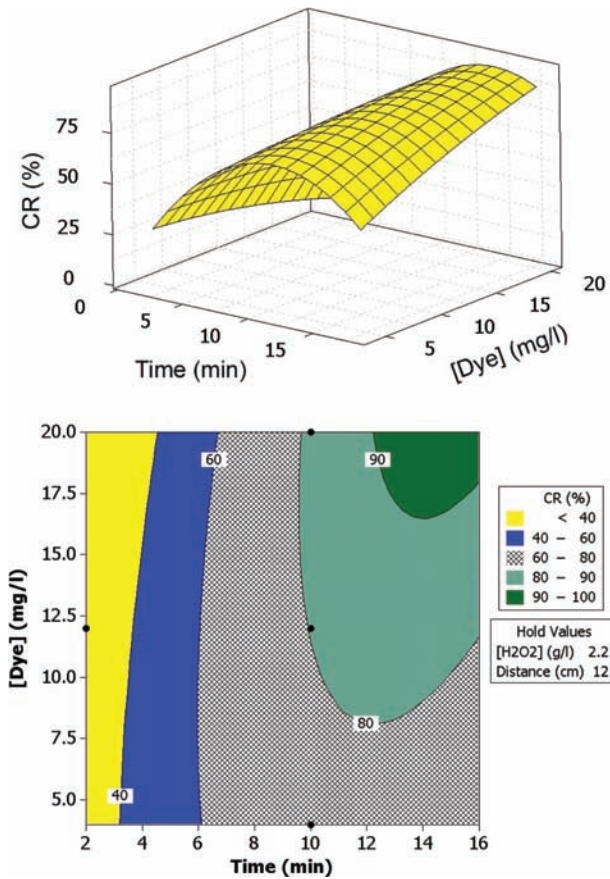


Fig. 3. The response surface and contour plots of the decolorization efficiency (%) as the function of reaction time (min) and initial dye concentration (mg/L).

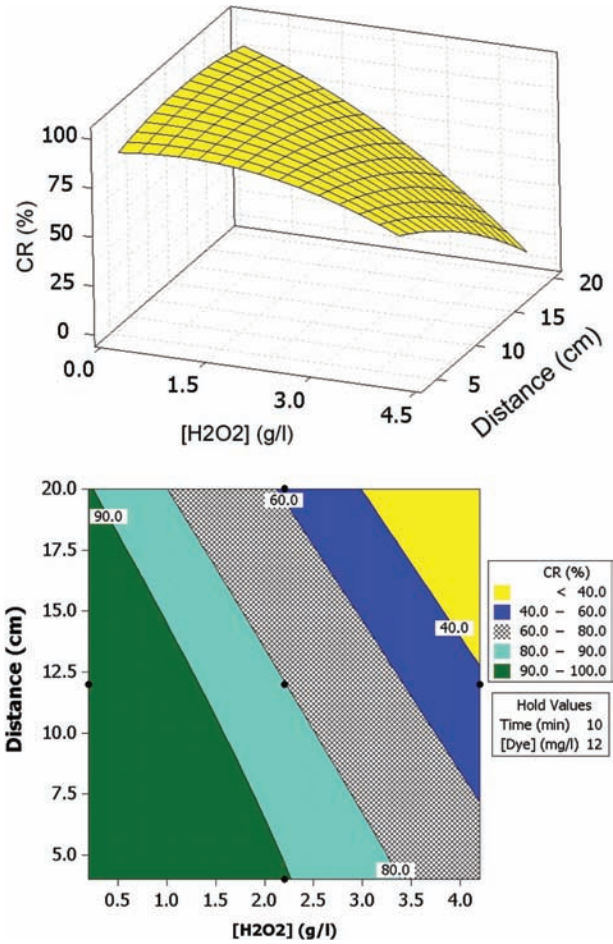


Fig. 4. The response surface and contour plots of the decolorization efficiency (%) as the function of initial H₂O₂ concentration (g/L) and the distance of UV lamp from the solution.

stant at 2.2 g/L, photooxidative decolorization efficiency was not changed considerably by increasing the initial dye concentration. It seems that up 10 min the effect of initial dye concentration on photooxidative decolorization efficiency is not obvious.

To study the effect of initial H₂O₂ concentration and distance of UV lamp from the solution on percent color removal, the experiments were carried out with initial H₂O₂ concentration varying from 0.2 to 4.2 g/L under different distance of UV lamp from the solution at constant initial dye concentration (12 mg/L) and reaction time (10 min). The results were displayed in Fig. 4. This Figure shows that the percent color removal slightly decreases with an increase in the amount of H₂O₂. The reason of this observation is thought to be the fact that hydroxyl radicals are consumed by hydrogen peroxide and many other species in solution and reach a steady-state concentration. At this point, when H₂O₂ is used in excess, hydroxyl radicals efficiently react with H₂O₂

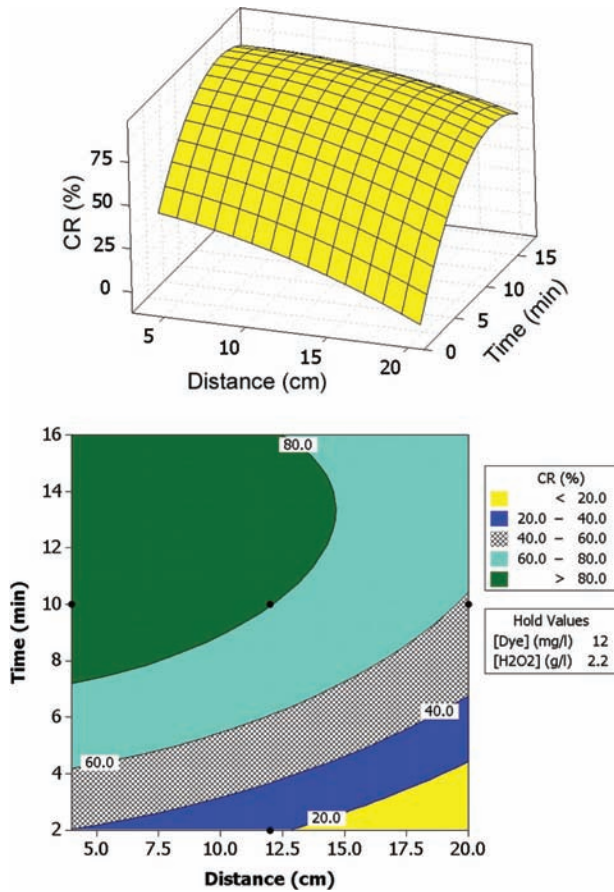


Fig. 5. The response surface and contour plots of the decolorization efficiency (%) as the function of reaction time (min) and the distance of UV lamp from the solution.

and produce hydroperoxy radicals ($\cdot\text{O}_2\text{H}$). Note that hydroperoxide radicals are less reactive than hydroxyl radicals [13, 17].

UV irradiation decomposes H_2O_2 to generate the hydroxyl radicals required for degradation of organic matters. The overall energy input to a photochemical process is related to the radiation intensity. The rate of degradation increases with increase in the radiation intensity. Figs. 4 and 5 show the percent color removal increased with decreasing the distance between UV lamp and the solution at all applied initial H_2O_2 concentrations studied. The reason of this observation is that the radiation intensity increased, from 8.0 to 21.9 W/m^2 , with decreasing the distance between UV lamp and the dye solution from 20 to 7.5 cm. Therefore percent color removal enhanced. The finding was in agreement with literature reports where higher radiation intensities would result in higher photooxidative removal efficiency [16, 37].

Fig. 6 shows the response surface and contour plots of the decolorization efficiency as a function of initial dye and H_2O_2 concentrations. A slightly improvement

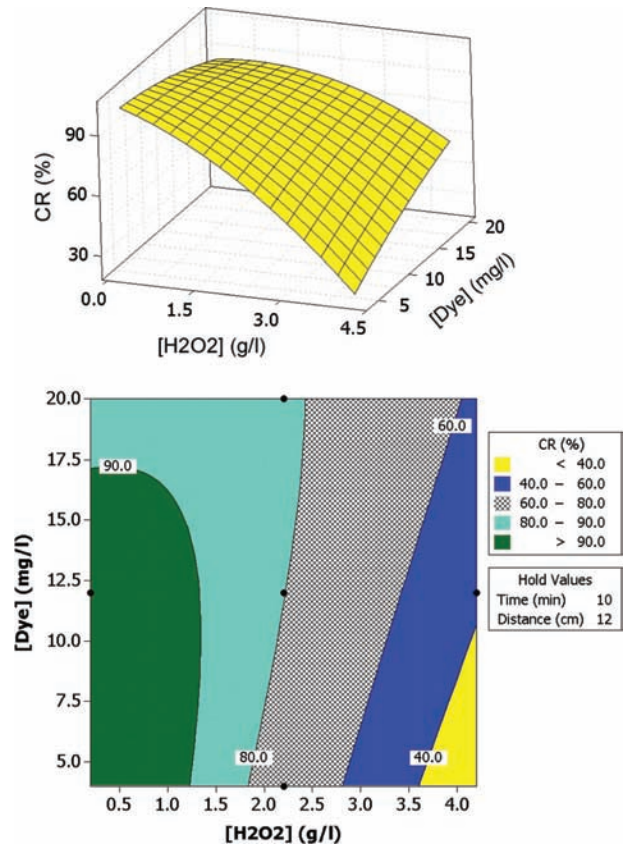


Fig. 6. The response surface and contour plots of the decolorization efficiency (%) as the function of initial dye (mg/L) and H_2O_2 (g/L) concentrations.

in photooxidation efficiency with increasing initial BR46 concentration has been observed. The reason of this observation is thought to be the fact that the increasing initial concentration of the dye increases the probability of reaction between dye molecules and oxidizing species. The finding was in agreement with literature reports where higher initial concentration of pollutant would result in higher photooxidative removal efficiency [11, 38]. In contrast, the percent color removal decreased with an increase in the amount of H_2O_2 as discussed previously.

3.5. Response optimization

The main objective of the optimization in this work is to determine the optimum values of variables for photooxidative decolorization using UV/ H_2O_2 process, from the model obtained using experimental data. The desired goal in term of decolorization efficiency was defined as “maximize” to achieve highest treatment performance. The optimum values of the process variables including

reaction time, initial dye concentration, initial H_2O_2 concentration and the distance from UV lamp for complete decolorization efficiency were 14 min, 20 mg/L, 1 g/L and 16 cm, respectively. After verifying by a further experimental test with the predicted values, the result indicated that the maximal decolorization efficiency was obtained when the values of each parameter were set as the optimum values, which was in good agreement with the value predicted from the model. It implies that the strategy to optimize the decolorization conditions and to obtain the maximal decolorization efficiency by CCD for the photooxidative decolorization of BR46 solution using UV/ H_2O_2 process is successful.

3.6. Kinetic model of critical effect of hydrogen peroxide

The kinetic model for decolorization of the dye was derived using the reaction mechanism in Eqs. (1–8). In this model two main steps are proposed to be responsible for removal: the formation of hydroxyl radicals ($\cdot OH$) as well as the formation of hydroperoxy radicals ($\cdot O_2H$) through reaction between H_2O_2 and $\cdot OH$. The reactions of $\cdot OH$ and $\cdot O_2H$ with dye molecules result in the formation of intermediates. These intermediates react with hydroxyl radicals to complete photooxidation. As it was previously reported, the Eq. (12) can be justified by considering the steady-state approximation for highly reactive intermediates such as $\cdot OH$ and $\cdot O_2H$ radicals in Eqs. (1–8) [13, 17]:

$$k = k_0 + \frac{bH}{1 + cH + dH^2}, \quad (12)$$

where H is the relative concentration of H_2O_2 expressed as the mass ratio of the H_2O_2 concentration to that of the dye at time zero ($H = \frac{[H_2O_2]_0}{[Dye]_0}$), k_0 is the photooxidation rate constant in the absence of H_2O_2 , b , c and d are the model parameters.

The apparent rate constants (k) of photooxidation of BR46 for each set of BR46- H_2O_2 combination were estimated by first-order kinetic assumption and from the slope of $\ln([BR46]/[BR46]_0)$ versus irradiation time. The sampling time intervals were 2 min in this section. Fig. 7 shows the predicted k values estimated from the kinetic model (solid line) and experimental ones as a function of $[H_2O_2]_0/[BR46]_0$. It can be seen that the model correctly predicts the trend of the photooxidative rate constants. Nonlinear curve-fitting (data-fitting) in the least-squares sense was performed using Matlab 6.5 mathematical software with optimization toolbox for windows. Sum of squares due to error (SSE) was used as the error function. This statistic measures the total deviation of the response

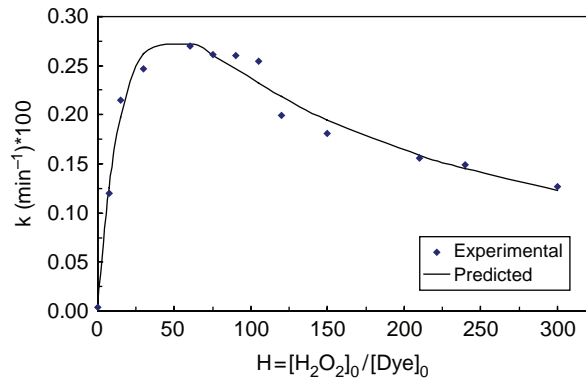


Fig. 7. Apparent rate constants, k , (min^{-1}), as a function of $H = [H_2O_2]_0/[BR46]_0$. The squares are the experimental values, whereas the solid line represents the predictions of the kinetics model. $\text{pH} = 7$, $I = 21.9 \text{ W/m}^2$, 100 mL treated, $[BR46]_0 = 20 \text{ mg/L}$.

values from the fit to the response values. It is also called the summed square of residuals and is usually labeled as SSE. It was computed with the following formula:

$$\text{SSE} = \sum_{i=1}^n (k_{\text{experimental}} - k_{\text{model}})^2, \quad (13)$$

where $k_{\text{experimental}}$ is the experimental values of apparent reaction rate constant (k (min^{-1})), k_{model} is the apparent reaction rate constant predicted by the model (Eq. (12)) and n is the number of data. A SSE value closer to zero indicates a better fit. SSE value and model parameters k_0 , b , c , and d were 0.0019, 0.0042 min^{-1} , 0.0201, 0.0315 and 0.0005, respectively.

From Fig. 7, it is also concluded that the rate of decolorization increased with increasing in H_2O_2 amount, but the improvement is not obvious above an optimum value. The reason of this observation was explained previously in section 3.4.

Fig. 8 shows a comparison between experimental and calculated values of k (min^{-1}), using the proposed kinetic model (Eq. (12)). We used two lines to show the success of the prediction. The one is the perfect fit (calculated data equal to experimental data), on which all the data of an ideal model should lay. The other line is the line that best fits on the data of the scatter plot with equation $Y = ax + b$ and it is obtained with regression analysis based on the minimization of the squared errors. The determination coefficient of this line is also presented (R^2). In Fig. 8, it is difficult to distinguish the best linear fit line from the perfect fit line, because the fit is so good. From these plots it can be seen that obtained results from the model are in good agreement with the experimental data.

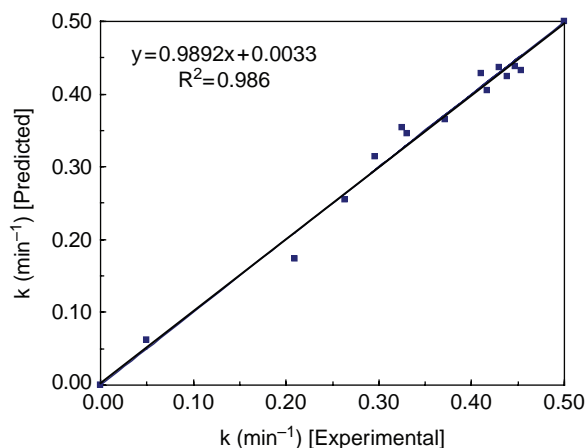


Fig. 8. Comparison between experimental and calculated apparent reaction rate constant, k , (min^{-1}). pH = 7, 100 mL treated, $I = 21.9 \text{ W/m}^2$, $[\text{BR46}]_0 = 20 \text{ mg/L}$.

3.7. Electrical energy efficiency

Since photooxidative removal of aqueous organic pollutants is an electric energy intensive process, and electric energy can represent a major fraction of the operating costs, simple Figures-of-merit based on electric energy consumption can be very useful and informative. According to the proposal of the Photochemistry Commission of International Union of Pure and Applied Chemistry (IUPAC), in the case of low pollutant concentrations, which applies here, the appropriate Figure-of-merit is the electrical energy per order (E_{EO}), defined as the number of kWh of electrical energy required to reduce the concentration of a pollutant by one order of magnitude (90%) in 1 m^3 of contaminated water. The E_{EO} ($\text{kWhm}^{-3} \text{ order}^{-1}$) can be calculated from the following equation [16, 17, 39]:

$$E_{\text{EO}} = \frac{P \times t \times 1000}{V \times 60 \times \log(C_i / C_f)}, \quad (14)$$

where P is the lamp power (kW) of the AOP system, t is the irradiation time (min), V is the volume (L) of the water in the reactor and C_i and C_f are the initial and final pollutant concentrations.

The electric energy ($\text{kWhm}^{-3} \text{ order}^{-1}$) required to decolorization of 20 mg/L of the dye from 100 ml dye solution in the optimized conditions was $41.2 \text{ kWhm}^{-3} \text{ order}^{-1}$. It is useful to relate the E_{EO} value found in this study to treatment costs. If the cost of the electricity, in Iran, is US\$ 0.023 per kWh, the contribution to treatment cost from electrical energy will be US\$ 0.95 per m^3 , for photooxidative treatment of BR46. In addition, the cost of hydrogen peroxide (30%, $d = 1.11 \text{ g/mL}$) required to decolorization of 20 mg/L of the dye from 100 ml dye solution in the optimized conditions was US\$ 38.22 per m^3 .

4. Conclusions

The results of this study demonstrate that CCD methodology could efficiently optimize the photooxidative decolorization of BR46 using UV/ H_2O_2 process. The optimum values of the reaction time, initial dye concentration, initial H_2O_2 concentration and distance of UV lamp from the solution were found to be 14 min, 20 mg/L, 1.0 g/L and 16 cm, respectively. Under optimal value of process parameters, high color removal (>95%) was obtained for dye solution containing BR46. Analysis of variance showed a high coefficient of determination value ($R^2 = 98.92\%$ and $\text{Adj-}R^2 = 97.79\%$), thus ensuring a satisfactory adjustment of the second-order regression model with the experimental data. Effect of experimental parameters on the decolorization efficiency was established by the response surface and contour plots of the model-predicted responses. The residuals follow a normal distribution.

The kinetic model, derived using the reaction mechanism of UV/ H_2O_2 process, provided good prediction of the photooxidative decolorization rate constant (k). The kinetic model is useful in estimating the desired H_2O_2 -to-dye ratio to prevent excess use of oxidant. The electrical energy consumption for photooxidative decolorization of BR46 solution was calculated and related to the treatment costs.

Acknowledgements

The authors gratefully acknowledge the research council of Azarbaijan University of Tarbiat Moallem for financial support.

References

- [1] F.I. Hai, K. Yamamoto and K. Fukushi, Hybrid treatment systems for dye wastewater, *Crit. Rev. Environ. Sci. Tech.*, 37 (2007) 315–377.
- [2] H. Al-Zoubi, S. Al-Thyabat and L. Al-Khatib, A hybrid flotation–membrane process for wastewater treatment: An overview, *Desalination and Water Treat.*, 7 (2009) 60–70.
- [3] A.R. Khataee, V. Vatanpour and A.R. Amani, Decolorization of C.I. acid blue 9 solution by UV/Nano- TiO_2 , Fenton, Fenton-like, electro-Fenton and electrocoagulation processes: A comparative study, *J. Hazard. Mater.*, 161 (2009) 1225–1233.
- [4] A.R. Khataee, V. Vatanpour and M. Rastegar, Remediation of the textile dye brilliant blue FCF from contaminated water by Fenton-Like Process: Influence of aromatic additives, *Turkish J. Eng. Environ. Sci.*, 32 (2008) 367–376.
- [5] A. Ozcan and A.S. Ozcan, Adsorption of Acid Red 57 from aqueous solutions onto surfactant-modified sepiolite, *J. Hazard. Mater.*, 125 (2005) 252–259.
- [6] F. Banat, S. Al-Asheh, R. Zomaout, B. Qtaishat, T. Alateat and S. Almayta, Photodegradation of methylene blue dye using bentonite as a catalyst, *Desalination Water Treat.*, 5 (2009) 283–289.
- [7] A.R. Khataee, M. Pourhassan and M. Ayazloo, Biological decolorization of C.I. basic green 4 Solution by microalga *Chlorella sp.*: Effect of operational parameters, *Chinese J. Appl. Environ. Biol.*, 15 (2009) 110–114.

- [8] A.R. Khataee and A. Khani, Modeling of nitrate adsorption on granular activated carbon (GAC) using artificial neuron network (ANN), *Int. J. Chem. Reactor Eng.*, 7 (2009) Article 5.
- [9] A.R. Khataee, M.N. Pons and O. Zahraa, Photocatalytic degradation of three azo dyes using immobilized TiO₂ nanoparticles on glass plates activated by UV Light Irradiation: Influence of dye molecular structure, *J. Hazard. Mater.*, 168 (2009) 451–457.
- [10] N. Daneshvar, A.R. Khataee, A.R. Amani Ghadim and M.H. Rasoulifard, Decolorization of C.I. acid yellow 23 solution by electrocoagulation process: Investigation of operational parameters and evaluation of specific electrical energy consumption (SEEC), *J. Hazard. Mater.*, 148 (2007) 566–572.
- [11] G. Devi, G. Kumar, M. Reddy and C. Munikrishnappa, Effect of various inorganic anions on the degradation of Congo Red, a di azo dye, by the photo-assisted Fenton process using zero-valent metallic iron as a catalyst, *Desalination and Water Treat.*, 4 (2009) 294–305.
- [12] J.J. Pignatello, E. Oliveros and A. MacKay, Advanced oxidation processes for organic contaminant destruction based on the fenton reaction and related chem., *Crit. Rev. Environ. Sci. Tech.*, 36 (2006) 1–84.
- [13] A.R. Khataee and H.R. Khataee, Photooxidative removal of the herbicide acid blue 9 in the presence of hydrogen peroxide: Modeling of the reaction for evaluation of electrical energy per order (E_{EO}), *J. Environ. Sci. Heal. B*, 43 (2008) 562–568.
- [14] N. Daneshvar and A.R. Khataee, Removal of Azo Dye C.I. acid red 14 from contaminated water using fenton, UV/H₂O₂, UV/H₂O₂/Fe(II), UV/H₂O₂/Fe(III) and UV/H₂O₂/Fe(III)/oxalate processes: A comparative study, *J. Environ. Sci. Health*, A 41 (2006) 315–328.
- [15] R. Andreozzi, V. Caprio, R. Marotta and D. Vogna, Paracetamol oxidation from aqueous solutions by means of ozonation and H₂O₂/UV system, *Water Res.*, 37 (2003) 993–1004.
- [16] M. Behnajady and N. Modirshahla, Evaluation of electrical energy per order (E_{EO}) with kinetic modeling on photooxidative degradation of C. I. acid orange 7 in a tubular continuous-flow photoreactor, *Ind. Eng. Chem. Res.*, 45 (2006) 553–557.
- [17] N. Daneshvar; A. Aleboye and A.R. Khataee, The evaluation of electrical energy per order (E_{EO}) for photooxidative decolorization of four textile dye solutions by the kinetic model, *Chemosphere*, 59 (2005) 761–767.
- [18] G.E.P. Box and K.B. Wilson, On the experimental attainment of optimum conditions, *J. R. Stat. Soc., Ser. B Stat. Methodol.*, 13 (1951) 1–45.
- [19] G.E.P. Box and W.G. Hunter, The 2k-p fractional factorial designs, *J. Technometrics*, 3 (1961) 311–458.
- [20] D.P. Obeng, S. Morrell and T.J.N. Napier, Application of central composite rotatable design to modeling the effect of some operating variables on the performance of the three-product cyclone, *Int. J. Miner. Process.*, 769 (2005) 181–192.
- [21] S.C.R. Santos and R.A.R. Boaventura, Adsorption modelling of textile dyes by sepiolite, *Appl. Clay Sci.*, 42 (2008) 137–145.
- [22] G.E.P. Box and D.W. Behnken, Some new three level designs for the study of quantitative variables, *J. Technometrics*, 2 (1960) 455–475.
- [23] X. Zhang, R. Wang, X. Yang and J. Yu, Central composite experimental design applied to the catalytic aromatization of isophorone to 3,5-xyleneol, *Chemometr. Intell. Lab. Sys.*, 89 (2007) 45–50.
- [24] G. Annadurai, R.S. Juang and D.J. Lee, Factorial design analysis for adsorption of dye on activated carbon beads incorporated with calcium alginate, *Adv. Environ. Res.*, 6 (2002) 191–198.
- [25] M. Ahmadi, F. Vahabzadeh, B. Bonakdarpour, E. Mofarrah and M. Mehranian, Application of the central composite design and response surface methodology to the advanced treatment of olive oil processing wastewater using Fenton's peroxidation, *J. Hazard. Mater.*, 123 (2005) 187–195.
- [26] E.C. Catalkaya and F. Kargi, Effects of operating parameters on advanced oxidation of diuron by the Fenton's reagent: A statistical design approach, *Chemosphere*, 69 (2007) 485–492.
- [27] A. Gursesam M. Yalcina and C. Dogarb, Electrocoagulation of some reactive dyes: A statistical investigation of some electrochemical variables, *Waste Manage.*, 22 (2000) 491–494.
- [28] T. Ölmez, The optimization of Cr(VI) reduction and removal by electrocoagulation using response surface methodology, *J. Hazard. Mater.*, 162 (2009) 1371–1378.
- [29] H. Cho and K.D. Zoh, Photocatalytic degradation of azo dye (Reactive Red 120) in TiO₂/UV system: Optimization and modeling using a response surface methodology (RSM) based on the central composite design, *Dyes Pigments*, 75 (2007) 533–543.
- [30] V.A. Sakkas, P. Calza, M. Azharul Islam, C. Medana, C. Baiocchi, K. Panagiotou and T. Albanis, TiO₂/H₂O₂ mediated photocatalytic transformation of UV filter 4-methylbenzylidene camphor (4-MBC) in aqueous phase: Statistical optimization and photoproduct analysis, *Appl. Catal., B* 90 (2009) 526–534.
- [31] M.B. Kasiri, H. Aleboye and A. Aleboye, Modeling and optimization of heterogeneous Photo-Fenton process with response surface methodology and artificial neural networks, *Environ. Sci. Technol.*, 42 (2008) 7970–7975.
- [32] A. Aleboye, N. Daneshvar and M.B. Kasiri, Optimization of C.I. Acid Red 14 azo dye removal by electrocoagulation batch process with response surface methodology, *Chem. Eng. Process*, 47 (2008) 827–832.
- [33] H.L. Liu and Y.R. Chiou, Optimal decolorization efficiency of Reactive Red 239 by UV/TiO₂ photocatalytic process coupled with response surface methodology, *Chem. Eng. J.*, 112 (2005) 173–179.
- [34] F. Harrelkas, A. Azizi, A. Yaacoubi, A. Benhammou and M.N. Pons, Treatment of textile dye effluents using coagulation–flocculation coupled with membrane processes or adsorption on powdered activated carbon, *Desalination*, 235 (2009) 330–339.
- [35] J. Seguro, N.S. Allen, M. Edge and A. Mc Mahon, Design of eutectic photoinitiator blends for UV/visible curable acrylated printing inks and coatings, *Prog. Org. Coat.*, 37 (1999) 23–37.
- [36] Y. Li, C. Chang and T. Wen, Application of Statistical Experimental Strategies to H₂O₂ Production on Au/Graphite in Alkaline Solution, *Ind. Eng. Chem. Res.*, 35 (1996) 4767–4771.
- [37] Y. Zang and R. Farnood, Photocatalytic decomposition of methyl tert-butyl ether in aqueous slurry of titanium dioxide, *Appl. Catal., B* 57 (2005) 275–282.
- [38] I.K. Konstantinou and T.A. Albanis, TiO₂-assisted photocatalytic degradation of azo dyes in aqueous solution, kinetic and mechanistic investigations, *Appl. Catal., B* 49 (2004) 1–14.
- [39] J.R. Bolton, K.G. Bircger, W. Tumas and C.A. Tolman, Fig-of merit for the technical development and application of advanced oxidation technologies for both electric and solar-derived systems, *Pure Appl. Chem.*, 73 (2001) 627–637.